13th World Conference on Earthquake Engineering
Vancouver, B.C., Canada
August 1-6, 2004
Paper No. 460

EVALUATION OF DYNAMIC PROPERTY AND SEISMIC PERFORMANCE OF LOW- AND MID-RISE RC BUILDINGS BASED ON MICROTREMOR MEASUREMENT

Narenmandula HO [1] and Hiroshi KAWASE [2]

SUMMARY

In this paper, first we measure microtremors of standard buildings in Kyushu University, most of which are low- and middle-rise reinforced concrete (RC) buildings to obtain resonant periods. Buildings of national universities had been constructed under strong code and budget control so they are expected to be similar to each other. Next, stiffnesses of the buildings are inverted from resonant periods together with design documents. Then we construct nonlinear seismic response models based on the numerical models already proposed for RC buildings in Kobe. Finally we conduct damage evaluation for these buildings by using simulated strong ground motions for a hypothesized Fukuoka earthquake. We confirmed that the resonant periods of buildings linearly correlate with their heights but that the long-span direction tends to have shorter resonant period than the short-span direction. The effects of soil-structure interaction are negligible in the short-span direction and noticeable in the long-span direction. We confirmed that the average seismic performance of measured buildings coincides with the average performance of buildings in Kobe and that no RC buildings will be collapsed or heavily damaged even for the worst scenario of expected earthquakes at the site.

INTRODUCTION

In 1995, the Hyogo-ken Nanbu Earthquake seriously damaged reinforced concrete (RC) structures in the urbanized area of Kobe. As major reasons of the damage to buildings in this earthquake, several factors are enumerated such as the lack of the strength of buildings designed in accordance with the older building code and the input motions to be stronger than expected on buildings [1]. However, middle and low-rise RC buildings are still used as offices, schools, apartment houses and the like, and there exist many poorly earthquake-resistant, decrepit buildings designed in accordance with the older building code. Therefore, from the view point of the safety measures against earthquakes in cities it is extremely important to analyze real seismic properties of such buildings and know their earthquake-resistance

[1] Graduate student, Kyushu University, Fukuoka, Japan, Email: mandora@seis.arch.kyushu-u.ac.jp
[2] Professor, Kyushu University, Fukuoka, Japan, Email: kawase@arch.kyushu-u.ac.jp

capacity. Especially, it is urgently required to establish the process to model the earthquake-resistance capacity of existing buildings based on actual measurement. Many studies have been performed to estimate the seismic properties of buildings at elastic stages based on the microtremor measurement, and the soil-structure interaction effects have also been studied [2]-[7]. However, we can hardly find studies to establish the analytic model of non-linear response based on actually measured seismic properties of buildings and thereby evaluate their safety margins against earthquakes.

In this study we tried to evaluate seismic properties of a group of middle and low-rise RC buildings as a whole, rather than to evaluate a property of each building, based on the microtremor measurement and evaluate their safety margins against earthquakes as a group of buildings from the estimated properties and the predicted strong motion. First, we analyzed microtremor records of the middle and low-rise RC buildings designed in accordance with the older building code and constructed in the Hakozaki Campus of Kyushu University and grasped their seismic properties. Next, we derived the mass and stiffness of the RC buildings from their design documents. On the assumption that the derived mass was correct, we inverted the actual stiffness in order that the theoretical resonant frequency correspons to the resonant frequency obtained through the microtremor observation. We obtained the ratios between the designed stiffness and the actual stiffness. Then, based on the assumption used by Nagato and Kawase [8], we established the nonlinear response models, conducted the earthquake response analyses, and verified the validity of the estimated yield strengths of the buildings. Finally, we inputted the strong motion of the hypothesized Fukuoka Earthquake at the Hakozaki Campus of Kyushu University to these models and evaluated their safety margins against earthquakes.

OUTLINE OF OBSERVATION AND METHOD OF ANALYSIS

Observed Building and Method of Observation

The location of the observation was in the Hakozaki Campus of Kyushu University, and the period of the observation was from July 16 through 19 in 2002. As the number of visitors to the buildings was small, the observation was conducted during the daytime. In total 22 RC buildings ranging from two-storied to six-storied were observed. Table 1 shows the outlines of the buildings such as names, sizes and shapes. Figure 1 shows the geological boring data near the sites of the targeted buildings.

The observation was conducted by installing one microtremor seismometer each on the free ground surface, each floor of the intermediate floors, and top floor or rooftop of the buildings. We deployed three microtremor seismometers in a triangular form only on the first floor. Figure 2 shows an example of the installation of microtremor seismometers (No. 8 building). Using SMAR-6A3P portable three-component accelerometer of Akashi with the amplifier of maximum amplification ratio of 10,000 times, we measured two sets of 15 minute data using a high cut filter frequency of 50 Hz and a sampling frequency of 100 Hz. The internal clock was corrected with the GPS time signal before starting the observation to ensure simultaneousness at every point.

Method of Analysis

The method of the analysis is as follows. First, we cut out a time segment of 40.96 seconds by overlapping 50% of data obtained from the microtremor measurement. Then, we obtained its Fourier Spectrum and Fourier Spectral Ratio and calculated the ensemble average for multiple segments. Next, we read from the Fourier Spectral Ratio between the top floor and the base (1F) the natural periods of the first peaks in the short-span direction (hereinafter referred to as ‘Top/Base・S’) and long-span direction (hereinafter referred to as ‘Top/Base・L’) of each building, respectively. In order to evaluate the soil-structure interaction effects, we also obtained from the first peak of the Fourier Spectral Ratio between the top floor and ground (GL) the natural periods in the short-span direction (hereinafter referred to as ‘Top/Grnd・S’) and long-span direction (hereinafter referred to as 'Top/Grnd·L') of the building in the same way. When it was difficult to select the peak among multiple peaks, we use, as supporting information, the fact that near the natural period the phase rapidly changes from around 0 degree to around 180 degrees and also the coherence decreases abruptly in order to determine the natural period. Figure 3 shows the amplitude, phase, and coherence of the Fourier spectral ratio for the Building No. 19 as an example.

Table 1 Outlines of the buildings such as names, sizes and shapes

No	Building name	Storey number	Basic structure	SS*SL (m)	Height (m)	H/SL	Built year	Form
1	207_Soundproof chamber of Agriculture	2F	Direct footing	10×41	8.3	0.8	1958	
2	126_Soundproof chamber of Engineering	2F	Direct footing	12×72	9.0	0.8	1960	
3	010_Development Center for Highet Education	2F	Direct footing	14×24	8.2	0.6	1927	
4	425_Coal Mining Materials	2F	Direct footing	14×22	8.2	0.6	1937	
5	136_Superconductor Science and Systems	2F	Direct footing	12×22	9.2	0.7	1931	
6	4041_Faculty of Human-Environment Studies	3F	Piled footing	15×27	10.8	0.7	1972	
7	4021Lecture room.1	3F	Piled footing	10×72	11.5	1.2	1957	
8	426_Clinicel Psychology and Human Development	3F	Piled footing	14×26	11.6	0.8	1988	
9	107_Faculty of Engineering(Function)	4F	Direct footing	9×82	14.0	1.6	1927	
10	105_Faculty of Human-Environment Studies	4F	Direct footing	15×20	16.6	1.1	1960	
11	104_Faculty of Engineering.4	4F	Piled footing	15×56	18.7	1.2	1966	
12	103_Faculty of Engineering.3	4F	Direct footing	15×60	14.9	1.0	1966	
13	108_Faculty of Engineering(Molecule)	4F	Direct footing	20×47	14.4	0.7	1963	
14	4022Lecture room.2	4F	Piled footing	10×31	14.5	1.5	1968	
15	075_The International Student Center	4F	Piled footing	12×25	15.1	1.3	1988	
16	002_Administration Bureau.2	5F	Piled footing	22×36	19.3	0.9	1979	
17	4042Faculty of Economics	6F	Piled footing	15×48	22.7	1.5	1980	
18	201_Faculty of Agriculture Bldg.1	6F	Piled footing	15×94	23.2	1.5	1969	
19	202_Faculty of Agriculture Bldg.2	6F	Piled footing	15×50	23.2	1.5	1967	
20	203_Faculty of Agriculture Bldg.3	6F	Piled footing	15×52	23.0	1.5	1965	
21	302_Faculty of Science Bldg.3	6F	Piled footing	15×75	22.6	1.5	1970	
22	031_Computer and Communications Center	6F	Piled footing	15×61	23.5	1.6	1970	

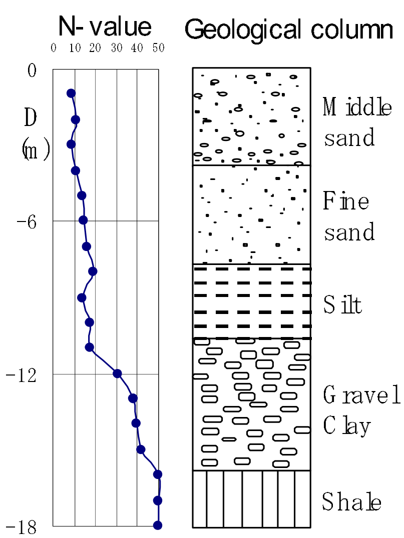

Fig.1 Geological boring data near the sites of the targeted buildings

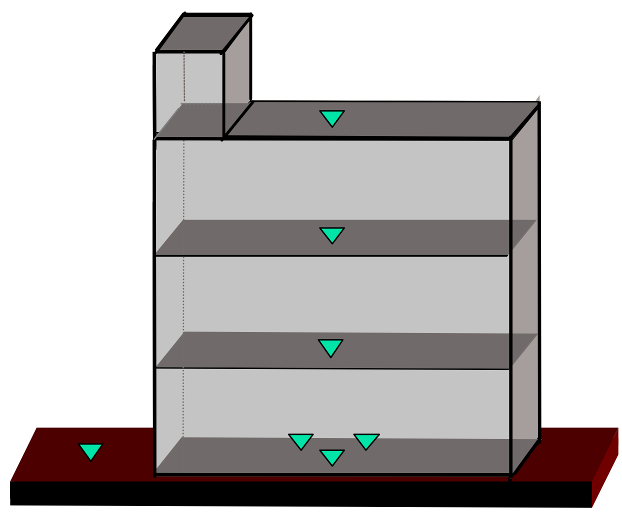

Fig. 2 An example of the installation of microtremor seismometers

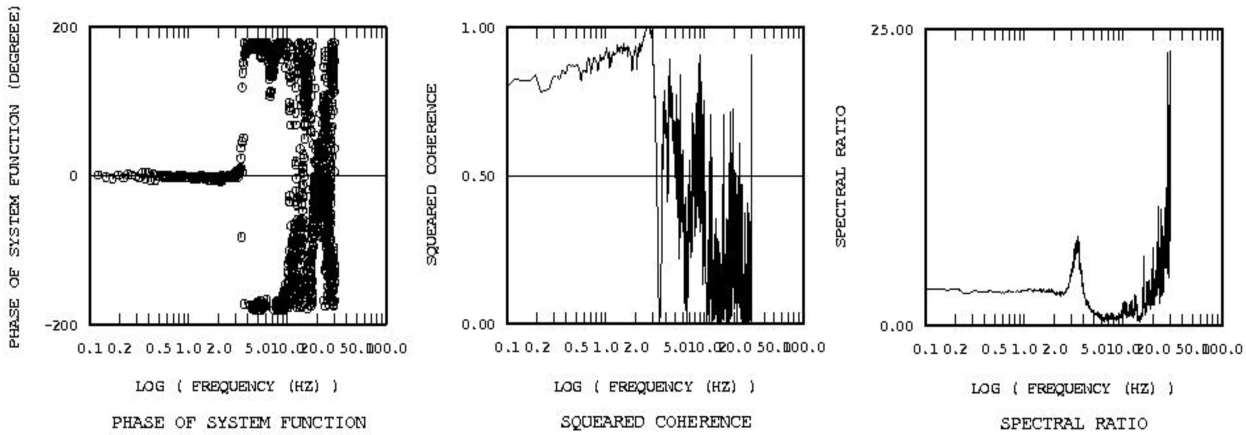

Fig. 3 Amplitude, phase, and coherence of the Fourier spectral ratio for the Building No. 19

EARTHQUAKE PROPERTY OF RC BUILDING WITH MICROTREMOR MEASUREMENT

Natural Period of RC Building

We can obtain the fundamental natural periods between the top floor and the base and between the top floor and the ground of the RC buildings from the result of the microtremor analysis. Table 2 shows the outlines of the observed buildings and their natural periods observed. Figure 4 shows the natural periods as a function of the number of stories of the observed buildings. As a whole, we can clearly recognize their dependence on height. Figure 5 shows the natural periods of the six-storied buildings with similar configurations in chronological order of construction. The newer buildings have shorter natural periods. The question whether it is caused by material deterioration or by changes in the design code or construction practice is a theme of our future study.

Comparison of Natural Periods in Short-Span Direction and Long-Span Direction

It is important to know the dynamic properties in the short-span direction and the long-span direction in grasping the main structural elements that contribute to the stiffness of the building. In addition, it is important to know a difference in stiffness between the two directions in estimating actual damage, since the building will be deformed much and become closer to be destroyed in the direction with weaker stiffness when it receives the same seismic motion from all directions. Therefore, we compare in Figure 6 the observed results of the 22 buildings for the natural periods of the short-span directions in the vertical axis and those of the long-span directions in the horizontal axis, which were derived from the Fourier Spectral Ratio of the Top/Base and the Top/Grnd. The straight lines on the figure are 1:1. Since the structural wall length per unit area in the short-span direction is larger than that in the long-span direction, the stiffness in the short-span direction is commonly considered to be larger than that in the long-span direction. However, as shown by the observed result of the top floor against the base (Top/Base), the natural period in the short-span direction is in almost all cases equal to or longer than that in the long-span direction except the Building No. 10. This suggests that the stiffness of the building in the short-span direction is relatively small provided that the influence of rocking is small. We can interpret why it is so as follows; the stiffness in the long-span direction is relatively large because its span is relatively short and they have many sidewalls and hanging walls attached. A similar report was also found in the past [9]. On the other hand, the comparison between the natural periods in the short-span direction and long-span direction derived from the Fourier Spectral Ratio of the top floor against the ground (Top/Grnd) varies widely, and we cannot find a certain tendency. This is so because the soil-structure interaction effect between the building and the ground is larger in the long-span direction as mentioned below.

Interaction Effects between Building and Ground

Regarding the earthquake response of the building, it is also important to appropriately evaluate the interaction between the building and the ground. In order to grasp the interaction effects between the building and the ground, we plot in Figure 7 the amplitude ratios between the top floor motion (nF) and ground (GL) motion of the building, between the rocking component multiplied by building height (Q*H) and the first floor motion, between the top floor motion and first floor motion (1F), and between the top floor motion and the first floor motion with rocking component corrected (1F+Q*H) (For physical meaning of this value see [3]-[6]). For each of these, one example is shown for each story in the short-span and long-span directions among all the buildings measured. These figures show that the resonant frequencies between the top floor motions and the first floor motions nF/1F are almost equal to those between the top floor motion and the rocking corrected first floor motion nF/(1F+QH). Therefore, we can conclude that the rocking movement of RC buildings in Kyushu University is so small that we can neglect the influence of rocking component to grasp the dynamic properties. We interpret that this is caused by the shapes of the buildings where the ratios between height and width are small as a whole, as shown on Table 1, so that sway motions are dominant. Figure 8 shows the ratios between the natural periods against the base (1F) and those against the ground as a function of the number of stories. This figure shows that the interaction effects between the middle and low-rise buildings and the ground are smaller in the short-span direction and larger in the long span direction. In addition, we can recognize in the long-span direction that, the more the number of stories is, the less the interaction effects with the ground tend to be. Figure 9 shows the interaction effects against the area of the building. Since the interaction effects in the short-span direction are not so clear as shown in Fig.8, their relation with the area is also not clear either. However, we can observe in the long-span direction that, the smaller the area is, the larger the interaction effects tend to be. Note that the influence of the number of stories is also included in this phenomenon. As shown in Figure 10, the influence of a difference between a piled footing and a direct footing of the building on the interaction effect is not clearly observed.

Table 2 Outlines of the observed buildings and their natural periods observed

No	Storey number	Building name	R_1F (sec)		R_G (sec)	
			SS	LS	SS	LS
1	2	207_Soundproof chamber of Agriculture	0.16	0.10	0.16	0.22
2	2	126_Soundproof chamber of Engineering	0.15	0.15	0.15	0.24
3	2	010_Development Center for Highet Education	0.16	0.15	0.17	0.16
4	2	425_Coal Mining Materials	0.17	0.17	0.16	0.16
5	2	136_Superconductor Science and Systems	0.15	0.15	0.18	0.15
6	3	4041_Faculty of Human-Environment Studies	0.15	0.16	0.16	0.17
7	3	4021Lecture room.1	0.15	0.14	0.17	0.26
8	3	426_ClinicelPsychology and Human Development	0.16	0.15	0.18	0.22
9	4	107_Faculty of Engineering(Function)	0.21	0.18	0.23	0.26
10	4	105_Faculty of Human-Environment Studies	0.22	0.28	0.22	0.29
11	4	104_Faculty of Engineering.4	0.23	0.22	0.23	0.22
12	4	103_Faculty of Engineering.3	0.21	0.22	0.21	0.22
13	4	108_Faculty of Engineering(Molecule)	0.22	0.19	0.23	0.19
14	4	4022Lecture room.2	0.27	0.19	0.30	0.25
15	4	075_The International Student Center	0.20	0.20	0.21	0.22
16	5	002_Administration Bureau.2	0.21	0.21	0.22	0.21
17	6	4042Faculty of Economics	0.28	0.22	0.30	0.25
18	6	201_Faculty of Agriculture Bldg.1	0.28	0.27	0.32	0.32
19	6	202_Faculty of Agriculture Bldg.2	0.31	0.30	0.35	0.35
20	6	203_Faculty of Agriculture Bldg.3	0.31	0.28	0.34	0.34
21	6	302_Faculty of Science Bldg.3	0.30	0.23	0.33	0.29
22	6	031_Computer and Communications Center	0.33	0.27	0.34	0.30

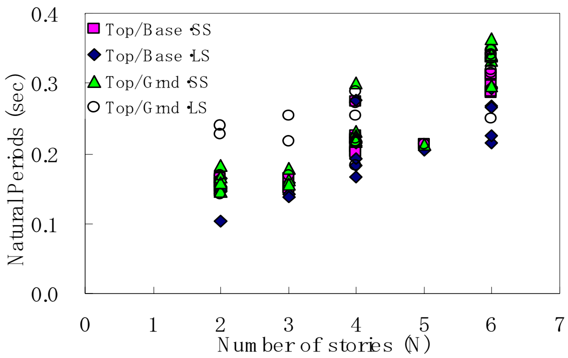

Fig. 4 Natural period versus stories number

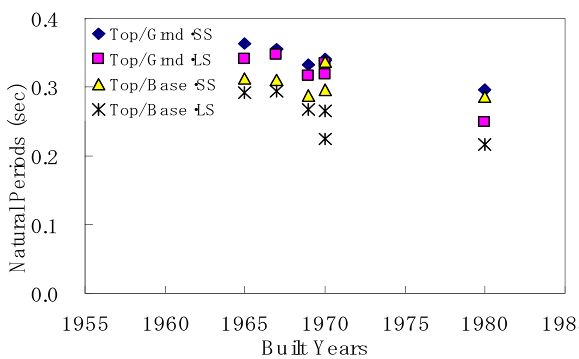

Fig. 5 natural period versus built year

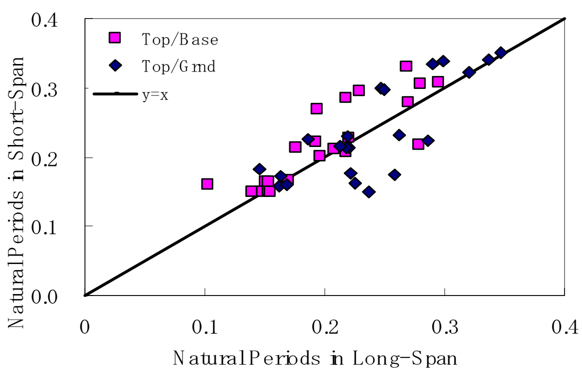

Fig. 6 Comparison of Natural Periods in Short Span Direction and Long Span Direction

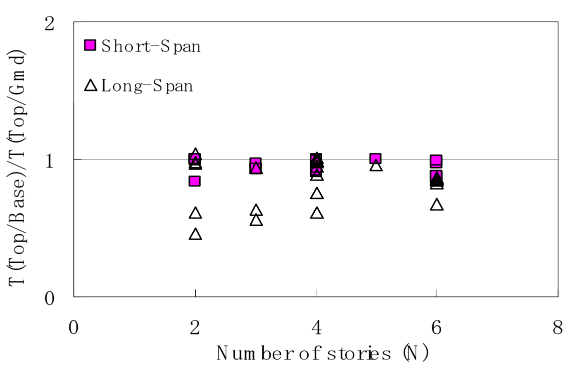

Fig. 8 Interaction to the Short-Span Direction and Long-Span Direction of a building

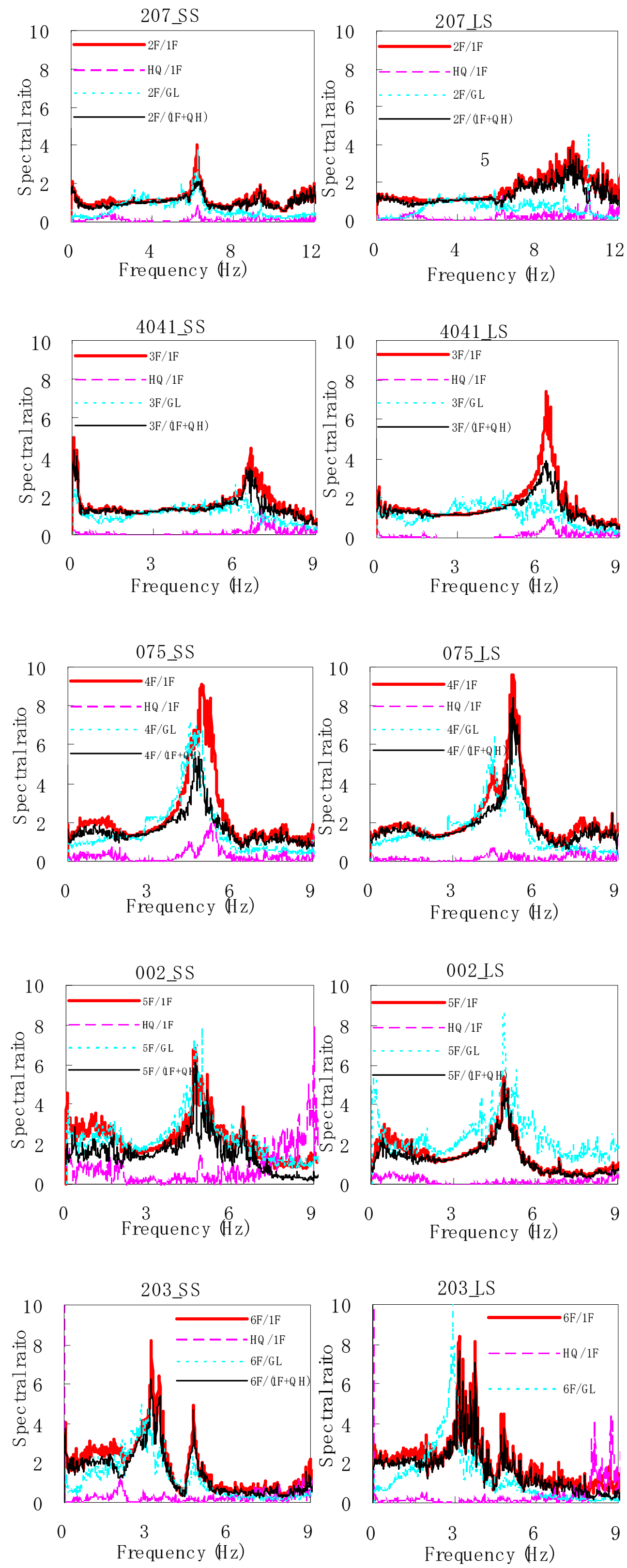

Fig. 7 Transfer functions obtained from microtremor observation

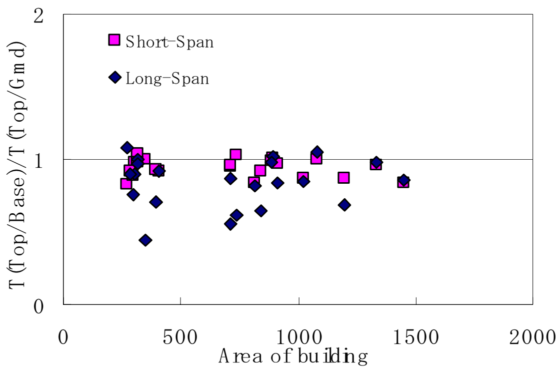

Fig. 9 Interaction effects against the area of each building

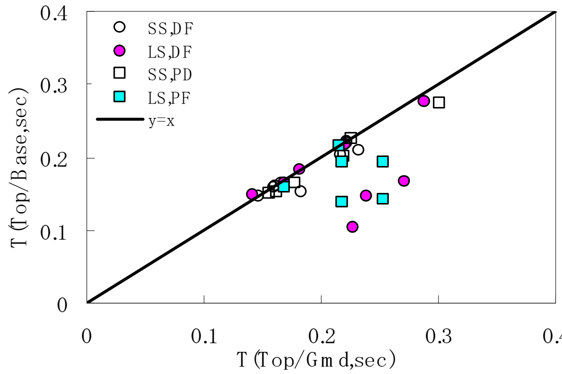

Fig. 10 Influence of the interaction of each building for different types of its foundation

ESTIMATION OF STRENGTH OF RC BUILDING

Estimation of Strength with Design Documents

We successfully got design calculation sheets and design drawings for 14 buildings among the 22 surveyed buildings. We read the heights of stories, weight, sizes and stiffness ratios of columns and beams, thickness of earthquake-resistant walls, and so on from them. Using the D-value method of Muto (horizontal force distribution coefficient method [10]), we obtained the stiffness of columns in the short-span direction and long-span direction of each floor of each building. Since it was difficult to find the stiffness of the earthquake-resistant wall accurately, we estimate the stiffness by using the n-times method in this study, i.e. the method to assume the D value of the earthquake-resistant wall to be n-times of the D value of the columns based on the dimension of the wall. Since some of the surveyed buildings have undergone several extensions, and some are rather old, we could not find sufficient design drawings for all of them. In these cases, we must admit that the difference between the stiffness of the columns evaluated from drawings and the stiffness of the actual building would be especially large.

Estimation of Strength with Microtremor Observation

For the purpose to estimate the actual stiffness of the building, we analyzed the actual value of the multi-degree-of-freedom system by stepping up by 0.0001 times the stiffness of the earthquake-resistant walls of each floor derived from the design drawings. The stiffness of the walls derived from the design drawings of the building contained only the stiffness of the earthquake-resistant walls considered in the seismic design, and the stiffness of sidewalls, partitioning walls, hanging walls, and wainscot walls was not included. In this paper, based on the assumption that an error in the estimated stiffness of the columns was small, all auxiliary stiffening effects by the rigid zones of side walls, partitioning walls, hanging walls, connections (panels) between columns and beams, and the increase in the column stiffness due to hanging walls and wainscot walls were represented by increased stiffness of earthquake-resistant walls. If the analyzed natural period equals the observed natural period derived from the Fourier spectral ratio between the top floor and base of the building from the microtremor measurement, we determine the stiffness to be the actual stiffness of the building. With this method, we inverted the stiffness in the long-span and short-span directions of each floor of the building. Table 3 shows the actual stiffness and the designed stiffness determined with the method mentioned above in the long-span and short-span directions of the building. The wall magnification factor in this table means the magnification factor against the stiffness of the earthquake-resistant wall at the time of design, which was required to equalize the natural period. However, it is not meaningful practically since the ratio becomes considerably large if the stiffness of the earthquake-resistant walls considered at the time of design are very small. We focus on the magnification factor with respect to the total stiffness combining the column stiffness and the wall stiffness at the time of design, rather than the wall stiffness only.

In the long-span direction of the building, the actual stiffness is 1.7 to 8.5 times the stiffness determined by the design drawings and 3.7 times on average. It varies largely. In the short-span direction, the actual stiffness is 1 to 5 times the stiffness determined by the design drawings and 2.1 times on average. The magnification in the long-span direction tends to be larger than that in the short-span direction, and the lower the building is, the larger the magnification tends to be. We consider this reflects the fact that in the lower-rise buildings, non-structural walls, which are not considered in the calculation in the design, contribute more than those in the higher-rise buildings. The fact that the magnification factor of the stiffness in the long-span direction is larger than that in the short-span direction is a direct consequence of the fact that the earthquake-resistant walls considered in the design are contained more in the short-span direction than in the long-span direction, and non-structural elements not considered in design, such as sidewalls, partitioning walls, hanging walls and wainscot walls are contained relatively more in the long-span direction than in the short-span direction. These influences are considered to largely depend on the plan of each building so that we should be careful to extend these averaged values to other types of buildings.

Table 3 Comparison of actual stiffness and designed stiffness

No	Bldg No	Floor	Long Span					Short Span				
			Actual stiffness	Designed stiffness	Wall magnification	Pillar+Wall magnification	Average magnification	Actual stiffness	Designed stiffness	Wall magnification	Pillar+Wall magnification	Average magnification
1	207	2F	4567	534	10.0	8.5		2081	899	3.0	2.3	
2	126	2F	2649	479	8.5	5.5		2748	1419	2.5	1.9	
3	4041	3F	4645	1432	4.6	3.2		4700	2186	2.5	2.2	
4	426	3F	9671	3600	3.4	2.7		5103	1485	3.5	3.4	
5	104	4F	12269	3768	5.1	3.3		8369	6488	1.4	1.3	
6	103	4F	7858	4683	2.0	1.7		8221	7836	1.1	1.0	
7	108	4F	3642	947	5.2	3.8	**3.7**	2528	1699	1.7	1.5	**2.1**
8	075	4F	3677	652	7.9	5.6		3355	676	5.7	5.0	
9	002	5F	14847	3279	5.2	4.5		11910	3477	4.1	3.4	
10	4042	6F	14417	5380	3.5	2.7		8516	5542	1.7	1.5	
11	201	6F	18911	6365	4.7	3.0		17150	8343	2.3	2.1	
12	202	6F	9628	4279	3.5	2.3		8377	7673	1.1	1.1	
13	203	6F	11183	5797	2.3	1.9		9546	7105	1.4	1.3	
14	302	6F	20759	7689	3.9	2.7		12665	7922	1.8	1.6	

Estimation Method of Yield Strength of Building with Earthquake Response Analysis

(1) Method of Establishing Building Model and Input of Seismic Motion

Using the obtained actual elastic stiffness, we establish the model of the RC buildings in Kyushu University. We refer to the Nagato-Kawase's "a set of building models" [8] here. The nonlinear property of the shear spring between two floors is the degrading tri-linear type [11], and the attenuation coefficient is set to be 5%. The shear strength of the building corresponding to the yield point is assumed to be the strength of the building. The initial stiffness is the actual stiffness determined previously by microtremors. The second branch stiffness is derived from the first stiffness and the ratio of the stiffness determined by referring to that of the Nagato-Kawase's model. The third stiffness (after yielding) is assumed to be 1/1,000 of the first stiffness. Regarding the criterion of heavy damage or collapse, we refer to the result of the experiment of RC columns [12][13] that the maximum strength is displayed at around the inter-floor deformation angle of 1/50 rad., and thereafter the strength decreases gradually to around 1/25 rad. Therefore, we assume that the model for which the maximum inter-floor deformation angle exceeds 1/30 rad. suffers at least heavy damage. This criterion of damage is assumed to be the same for older buildings constructed in accordance with the older building code before 1981 and for newer buildings constructed in accordance with the current building code after 1981. The nonlinear response of the model is calculated by using the Newmark's β-method [14], where we set β=1/4 and time span t = 0.005 s. The seismic motion is inputted at the base (i.e., no soil-structure interaction is considered). We established 28 building models consisting of 14 short-span direction models and 14 long-span direction models with two to six floors. We input two horizontal components of seismic motions to the model of each direction of each building, and we assume that the building suffers at least heavy damage when the maximum inter-floor deformation angle exceeds 1/30 rad. by either component of the strong motion. Figure 11 shows, as an example, a conceptual drawing of the analytic model and nonlinear property of the Building No. 11 in the long-span direction.

We used the synthetic waves [15] of the Hyogo-ken Nanbu Earthquake as the input seismic motions. They estimated first the four asperity source model that can reproduce the observed waves containing the pulse-like velocity waveforms with the predominant period of around one second and then conducted the wave propagation simulation with the three-dimensional basin structure that can consider the "edge effect". As a result, they could reproduce the observed record quite well and succeeded in generating the high-velocity amplification area corresponding to the earthquake disaster belt. In this study, we decided to use 2,606 waves at Nada-Ward and Higashi Nada-Ward among the reproduced waves of the Hyogo-ken Nanbu Earthquake.

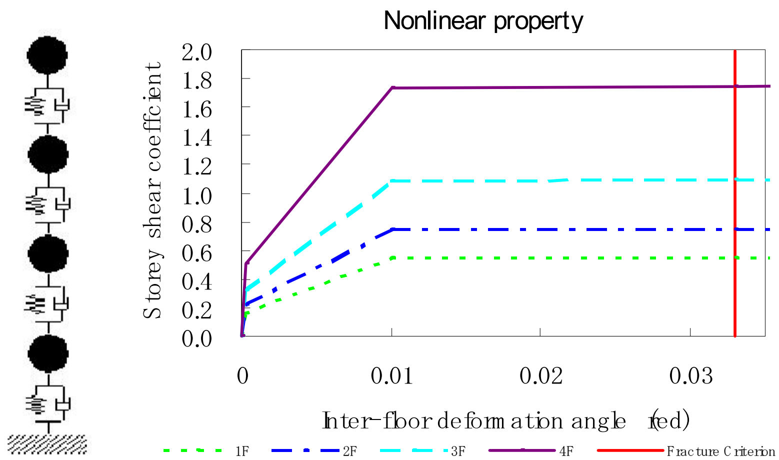

Fig. 11 Conceptual drawing of the analytic model and nonlinear property

(2) Verification Method of Yield Strength of Building

When we estimate the strength of a building, it is important to estimate its actual yield strength at the time when such building suffers damage in a large earthquake. In this study, first we set the actual stiffness as the initial (i.e., elastic) stiffness, which explained the observed natural period. Then, we established the building model from the initial stiffness, the assumed ratio of the second branch stiffness and the displacement of the yield point. To verify whether the assumed strength of this model was appropriate or not, we compared it with the Nagato-Kawase model [8], which had already been verified with the observed damage ratios during the Hyogo-ken Nanbu Earthquake. We thereby evaluated the equivalent yield strengths in terms of the Nagato-Kawase model. In establishing the Nagato-Kawase model, they conducted the earthquake response analysis with the reproduced strong motions of Matsushima and Kawase and completed a set of models for standard RC buildings with three-stories, six-stories, nine-stories, and twelve-stories. They proved that the proposed set of models can reproduce the observed damage ratios derived from the building damage statistics. When they estimate the yield strength of models they introduced variations to the yield strength of the buildings. They adopted the logarithmic normal distribution of λ= 0.0095 and ζ= 0.423 that had been determined by Shibata [16] based on the research of the strengths of buildings after the Miyagi-ken Oki Earthquake of 1978.

In this paper, we first established the Nagato-Kawase building models for two-stories, four-stories, and five-stories based on the data of the Nagato-Kawase building models for three-stories and six-stories. By inputting the 2,606 reproduced waves of the Hyogo-ken Nanbu Earthquake by Matsushima and Kawase [15] to the Nagato-Kawase building models ranging from two-stories to six-stories, we calculated the ratios of heavy damage or collapse (hereinafter referred to as simply ‘the damage ratio’) for each of the 12 buildings with different strengths with a log-normal distribution (12 is the number of bins for log-normal probabilistic density). Then we determined the probabilistic density distribution function (with logarithmic normal distribution) conforming to the damage ratios for these 12 buildings with different strengths. Figure 12 shows the calculated damage ratios and probabilistic density distribution functions obtained for the buildings with two-stories to six-stories. At the same time, we calculated the damage ratio of each building in Kyushu University by inputting the same 2,606 reproduced waves of the Hyogo-ken Nanbu Earthquake to the building models presented in this paper. By comparing these damage ratios to the probabilistic damage density functions of the Nagato-Kawase building models, we estimated the equivalent yield strength of the buildings in Kyushu University.

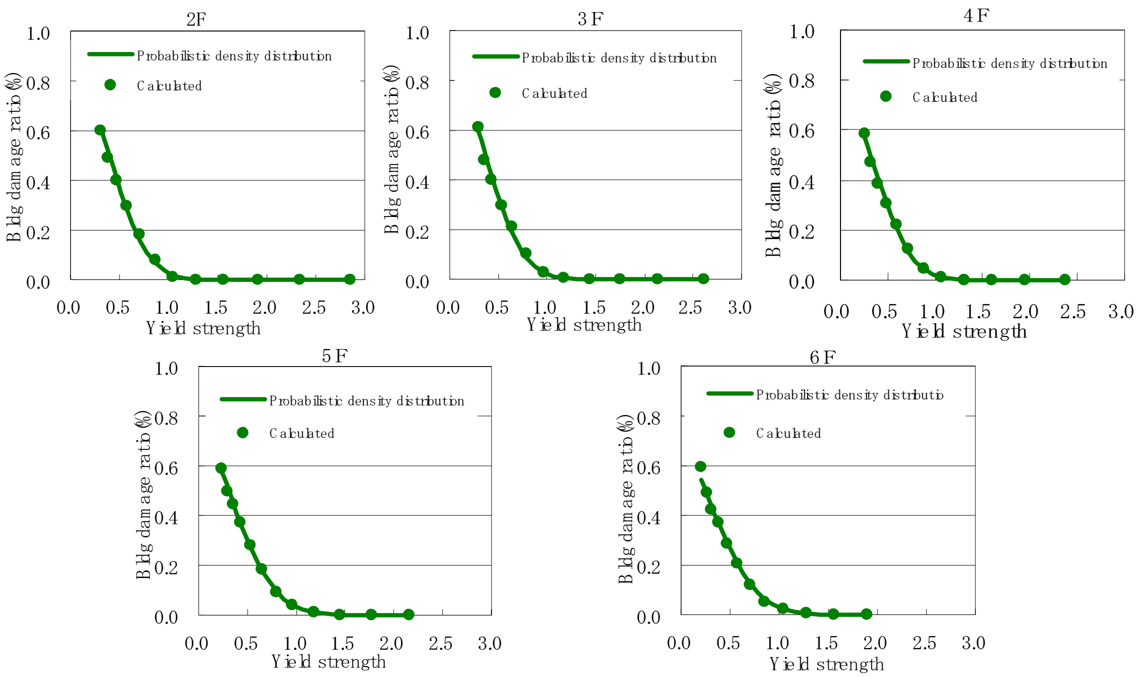

Fig. 12 Calculated damage ratios and probabilistic density distribution functions obtained for the buildings with two-stories to six-stories

(3) Result of Estimation of Strength of Building

By inputting the same strong motions to the Nagato-Kawase models and to the building models presented in this paper, we calculated the damage ratios of heavy damage or collapse, and then we considered to have the equivalent yield strength of the buildings if the same damage ratios can be obtained. The result is as follows: the yield strength of the two-storied buildings in Kyushu University is equal to that of two-storied buildings in Kobe on average; the yield strength of the three-storied and four-storied buildings in Kyushu University is slightly smaller than that of three-storied and four-storied buildings in Kobe; and the yield strength of the five-storied and six-storied buildings in Kyushu University is slightly larger than that of five-storied and six-storied buildings in Kobe. As a whole, it can be said that the yield strength of the middle and low-rise RC buildings in Kyushu University is almost equal to that of middle and low-rise RC buildings in Kobe on average, which were heavily damaged in the Hyogo-ken Nanbu Earthquake. Table 4 shows the estimated yield strength of the buildings in Kyushu University and that of standard RC buildings in Kobe as the base shear coefficient. Figure 13 shows the comparison between the estimated yield strength of the RC buildings in Kyushu University and that of the standard RC buildings in Kobe. Since there were only two RC buildings in this measurement designed after 1981 in accordance with the current building code, we show their yield strength only for reference. Their yield strength is slightly larger than that of buildings constructed in accordance with the older building code, but quite smaller than that of new buildings in Kobe.

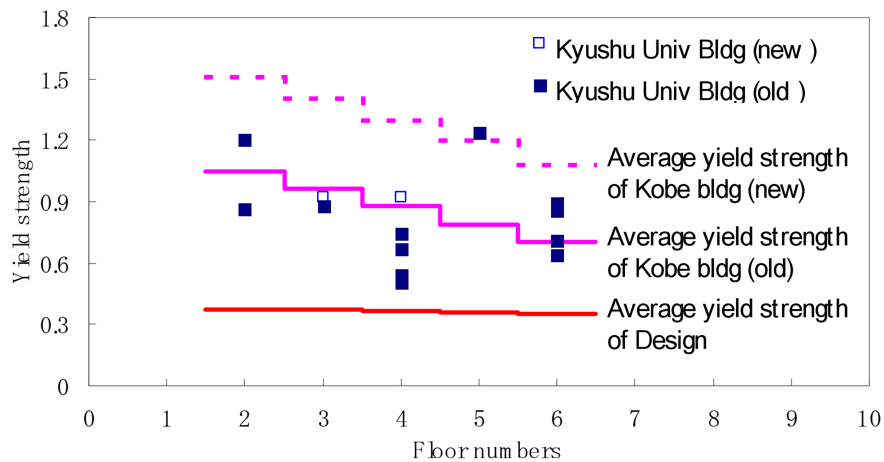

Fig. 13 Comparison between the estimated yield strength of the RC buildings in Kyushu University and that of the standard RC buildings in Kobe

Table 4 Comparison of estimated yield strength of the buildings in Kyushu University and that of standard RC buildings in Kobe as the base shear coefficient

No	Bldg NO	Floor	Yield strength Short Span	Yield strength Long Span	Yield strength	Yield strength of kobe bldg
1	207	2F	0.86	2.20	0.86	1.05
2	126		1.20	1.29	1.20	
3	426	3F	0.92	1.24	0.92	1.41 (new)
4	4041		1.27	0.88	0.88	0.96
5	104	4F	0.62	0.54	0.54	0.88
6	103		0.84	0.67	0.67	
7	108		0.75	1.17	0.75	
8	075		0.92	1.05	0.92	1.30 (new)
9	002	5F	1.35	1.24	1.24	0.79
10	4042	6F	0.87	1.74	0.87	0.70
11	201		0.89	1.02	0.89	
12	202		0.68	0.64	0.64	
13	203		0.71	0.99	0.71	
14	302		0.86	1.53	0.86	

The equivalent strength obtained by above procedure is determined at the tail of the probabilistic density function as shown in Figure 12 when the strength is 0.8 and larger. To verify its appropriateness, we also tried to determine it with the damage rate obtained by inputting the strong motion of 1.5 times the reproduced strong motion of the South Hyogo Earthquake and obtained an estimated margin of error of the yield strength between 0.001 and 0.171. Therefore, we consider that we have obtained the yield strength quite accurately.

ESTIMATION OF DAMAGE OF RC BUILDING

Nakamichi and Kawase [17] assumed that the fault rupture equivalent to that of the Hyogo-ken Nanbu Earthquake, one of the largest destructive earthquakes that we had ever experienced, would occur on the

Kego Fault, which is lying directly underneath Fukuoka City. They conducted a broadband strong motion prediction for this hypothesized earthquake, using the hybrid method combining the statistical Green's function method [18] and the three-dimensional finite difference method [19]. They assumed four scenarios by varying the locations and depths of four asperities and the rupture starting point. By inputting the strong motion at the location of Kyushu University estimated by Nakamichi and Kawase to the building models established in this paper, we predicted the seismic damage of the buildings in Kyushu University. Figure 14 shows the peak ground velocity distributions of the earthquakes of the four scenarios. The location of Kyushu University is marked with a square in the figure. Figures 15 to 18 show the maximum inter-floor deformation angles of the surveyed buildings in the forth scenario that gives the largest peak ground velocity. This result shows that even if the Kego Fault ruptures, the middle and low-rise RC buildings in Kyushu University will not suffer either heavy damage nor collapse.

To grasp the situation when the RC buildings in Kyushu University suffer heavy damage, we calculated the damage by inputting the strongest seismic motion among the reproduced Matsushima-Kawase strong motions during the Hyogo-ken Nanbu Earthquake. As a result, with the strongest seismic motion, nine among the fourteen buildings were estimated to suffer at least heavy damage. Figures 19 and 20 show the maximum inter-floor deformation angle in the short-span and long-span directions of the buildings in Kyushu University with the strongest seismic motion. We have found that, when suffering heavy damage, most of the buildings collapse at first or second floors, and more buildings are destroyed in the short-span directions than in the long-span directions. The reason why lower floors are easily destroyed is presumed that first floors have more openings such as doors and hinged double doors than upper floors, and large spaces such as laboratories are often placed there. Therefore, the shear strength coefficient at the base is relatively small. The fact that the possibility of destruction in the short-span direction is larger than that in the long-span direction is a direct consequence of the fact that the stiffness and strength estimated from the proposed procedure here are relatively small in the short-span direction.

The reason why the buildings of Kyushu University do not suffer heavy damage by the supposed seismic motion at the site is that the peak ground velocity at the location of Kyushu University by the Fukuoka Earthquake assumed by Nakamichi and Kawase does not exceed 82 cm/sec and is significantly smaller than the maximum reproduced peak ground velocity of 124 cm/sec of the Hyogo-ken Nanbu Earthquake since Kyushu University is located at about 6 km away from the Kego Fault, and the ground directly underneath the university is relatively firm. Figure 21 shows the spectra of the predicted wave of the Fukuoka Earthquake and the maximum reproduced wave of the Hyogo-ken Nanbu Earthquake. We see noticeable amplitude difference in the important period around 1 to 2 second, which corresponds to the predominant period of post-yield condition of row- and middle-rise RC buildings.

CONCLUSION

In this paper, first we conducted the spectral analysis of the 22 middle and low-rise RC buildings in Kyushu University for microtremor data. Since the interaction effects between the buildings and the ground including the rocking are small, we determined the natural period of buildings with the Fourier spectral ratio between the top floor and the base. We have found the followings: 1) the obtained natural period becomes longer when the buildings become taller; 2) it tends to become shorter when the buildings become newer; 3) the natural period in the short-span direction of the buildings is almost equal to or slightly larger than that in the long-span direction; 4) the interaction effects with the ground are small in the short-span direction and noticeable in the long-span direction; and 5) taller buildings and those with bigger floor spaces have smaller interaction effects with the ground. In this measurement, we could not find a difference in the soil-structure interaction effects for different types of foundations.

Next, from the design drawings and design calculation sheets, we derived the designed stiffness of the

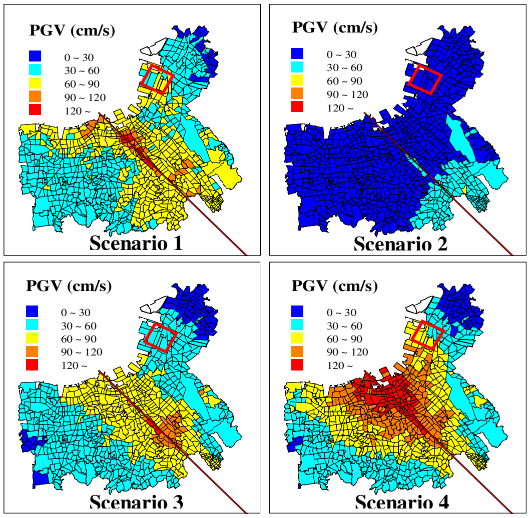

Fig. 14 Peak Ground Velocity distributions calculated for four rupture scenarios in Fukuoka

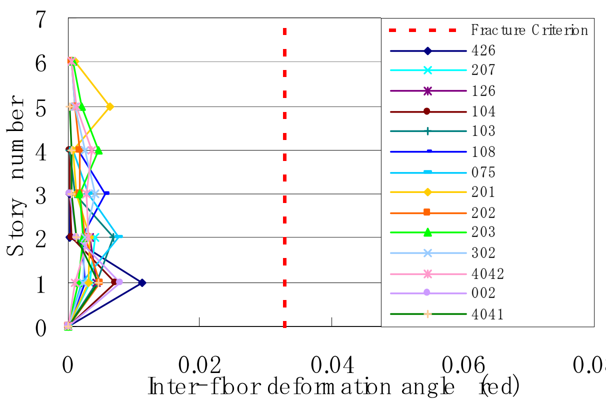

Fig.15 Maximum inter-floor deformation angles of the buildings(Long Span) by the Fukuoka Earthquake ground motions (NS) assumed

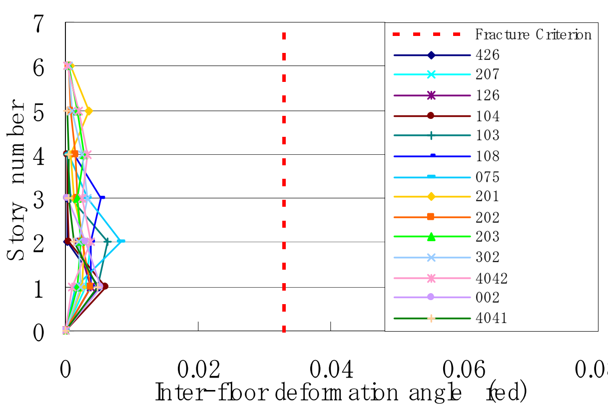

Fig.16 Maximum inter-floor deformation angles of the buildings(Long Span) by the Fukuoka earthquake ground motions (EW) assumed

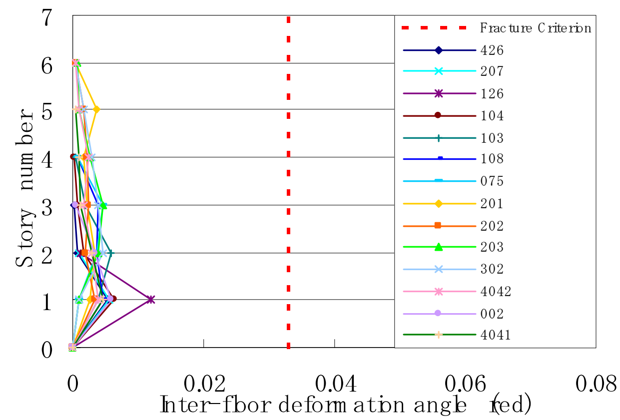

Fig.17 Maximum inter-floor deformation angles of the buildings(Short Span) by the Fukuoka earthquake ground motions (NS) assumed

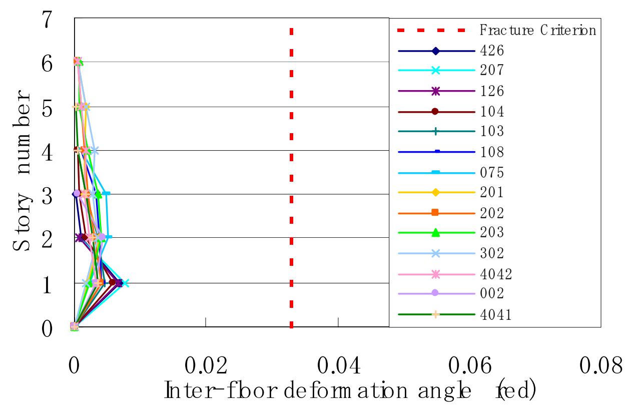

Fig.18 Maximum inter-floor deformation angles of the buildings(Short Span) by the Fukuoka earthquake ground motions (EW) assumed

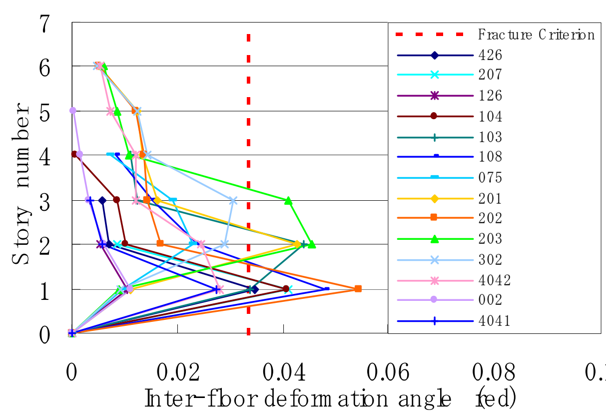

Fig.19 Maximum inter-floor deformation angles of the buildings(Long Span) by the Hyogo-ken Nanbu earthquake maximum ground motion

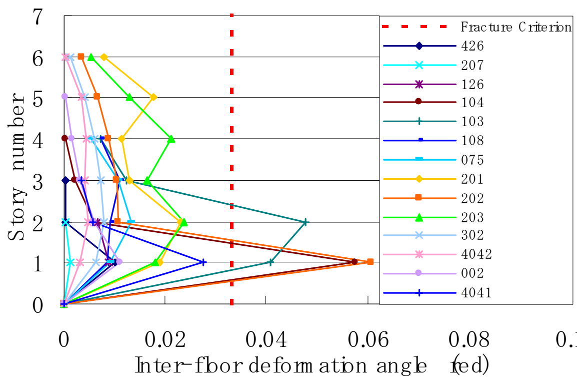

Fig.20 Maximum inter-floor deformation angles of the buildings(Short Span) by the Hyogo-ken Nanbu earthquake maximum ground motion

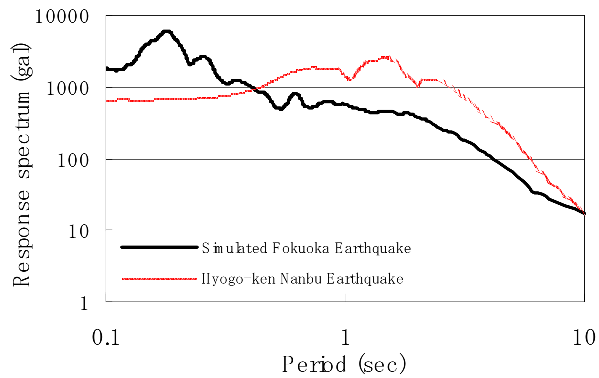

Fig. 21 Spectra of predicted wave of Fukuoka earthquake and the maximumr eproduced wave of Hyogo-ken Nanbu earthquake

columns and earthquake-resistant walls both in the short and long-span directions of each floor of the buildings. Then, by gradually increasing the designed stiffness of the earthquake-resistant walls, we conducted the eigen value analyses and estimated the actual stiffness of the building by matching the natural periods of models with the observed ones. As a result, the actual stiffness was found to be 2.1 times the designed stiffness in the short-span direction on average and 3.7 times the designed stiffness in the long-span direction. Based on this actual stiffness and the assumptions that Nagato and Kawase had established, we constructed nonlinear shear response analysis models and obtained the equivalent yield strengths of the RC buildings in Kyushu University by comparing their damage ratios with the damage ratios of the Nagato-Kawase model. As a result, we found: 1) those of the two-storied buildings were almost equal; 2) those of the three and four-storied buildings were smaller by approximately 20%; and 3) those of the five and six-storied buildings were larger by approximately 10%. Since the average yield strength of the buildings as a whole is almost equal to that of the RC buildings in Kobe, the yield strength of the buildings modeled in this paper is considered to be valid for damage evaluation.

Finally, we estimated the damage using the building models thus established and the strong motion of the hypothesized Fukuoka earthquake which may occur in Fukuoka in the future. We predicted that the Fukuoka earthquake could not heavily damage the RC buildings in Kyushu University. This is because the surveyed buildings are located away from the fault, and the ground under the buildings is relatively firm. However, if the RC buildings in Kyushu University are subject to the ground motion as strong as in Kobe, nine out of fourteen buildings will be destroyed at first or second floors. The result of the comparison between the short-span direction and the long-span direction shows that the buildings will be destroyed more in the short-span direction. It directly reflects the observed fact that the actually measured natural period is relatively longer in the short-span direction. However, the question whether lower natural period immediately means that the yield strength is also lower, as assumed in this paper, have to be studied further.

ACKNOWLEDGEMENT

This study was partially supported by the Special Coordination Funds of the Ministry of Education, Culture, Sports, Science and Technology, Japan (P.I.: Kojiro Irikura of Kyoto University).

REFERENCES

1. AIJ (1997) “Report on the Hanshin-Awaji Earthquake Disaseter” Building Series Volume 3, AIJ.

2. Imaoka, k. and T. seike (1996) Seismic Response Evaluation of a Structure with surface Ground Through Microtremor Measurement, *J. Struct. Constr. Eng*., AIJ, 490, 101-110.
3. Fukuwa, N. G. M. Ali, S. Yagi (1995) A Study on the Effect of Soil Structure Interaction on the Eigenproperty of Structure, *J. Struct. Constr. Eng*., AIJ, 475, 35-44.
4. Hikita, T. Y. Naito, A. Niousha, H. Harada (2003) Dynamic characteristic estimation of buildings during microtremors considering rocking motion of the base, *J. Struct. Constr. Eng*., AIJ, 566, 37-44
5. Haraguchi, K. J. Kanda, M. Inagaki (2003) A method for identification of multistoried buildings considering soil-structure interaction by microtremor observation, *J. Struct. Constr. Eng*., AIJ, 564, 31-37.
6. Matsuyama, C. N. Fukuwa, J. Tobita (2001) Dynamic characteristics of adjacent low and medium-rise buildings based on earthquake observation, forced vibration experiment and microtremor observation, *J. Struct. Constr. Eng*., AIJ, 545, 87-94.
7. Yagi, S. N. Fukuwa, J. Tobita (2002) Influence of rotational foundation input motion due to rayleigh wave on transfer function estimation of low-rise r.c. buildings based on microtremor observation, *J. Struct. Constr. Eng*., AIJ, 552, 77-84.
8. Nagato, K. and H. Kawase (2004) Damage Evaluation Models of Reinforced Concrete Buildings Based on the Damage Statistics and Simulated Strong Motions During the 1995 Hyogo-ken Nanbu Earthquake, *Earthq. Eng. Struct. Dyn.* (in press).
9. Ooba, S. (1978) Dynamic Property of Multi-Family Housing Based on Microtremor Measurement, Proceedings., JAEE, 5th,1153-1159.
10. Takefuzi, K (1963) Earthquake-proof calculating method, *Maruzen*.,
11. Fukada, Y (1969) Hysteresis characteristic of Reinforced Concrete Building (Part1) Setup and Response Calculation of Degrading Stiffness Tri-Linear Model , *Proc. of 46th Kanto Chapter Architectural Research Meeting*, AIJ, 121-124.
12. Hirohashi, E. H. Fukuyama, S. Nakazawa, K. Kokubun, H. Hiraishi (1996) Structural Performances of RC Colums Planed to Prevent Decreasing of Strength After Shear Failure Part1. Outline and Investigations by Lateral Reinforcement Ratio, *Proc. of the Annual Meeting of AIJ,* Structures Ⅳ,C-2, 237-238.
13. Nakamoto, N. A. Tyou, T. Yoshioka, O. Mori (1996) Development of High-rise Reinforced Concrete Building [Towers-31] (Part 4 Loading Tests of Column Element), *Proc. of the Annual Meeting of AIJ,* Structures Ⅳ,C-2, 777-778.
14. Shibada, A (1981) Newest Earthquake-resistant Construction Analysis, Morikita Shuppan Co., Ltd.
15. Matsushima, S. and H. Kawase (2000) Multiple asperity source model of the Hyogo-ken Nanbu earthquake, *J. Struct. Constr. Eng*., AIJ, 534, 33-40.
16. Shibata, A. (1980) Prediction of the Probability of Earthquake Damage to Reinforced Concrete Building Groups in a City, the 7th World Conference of Earthquake Engineering, Vol. 4, 395-402.
17. Nakamichi, S. and H. Kawase (2002) Broadband Strong Motion Simulation in Fukuoka City Based on a Three-dimensional Basin Structure and a Hybrid Method, *J. Struct. Constr. Eng*., AIJ, 560, 83-91.
18. Ito, S., H. Kuhara, and H. Kawase (2001) Calibration of Strong Motion Prediction Method Using Statistical Green's Function and its Application to Hypothesized Fukuoka Earthquake, *J. Struct. Constr. Eng*., AIJ, 540, 57-64.
19. Graves, R.W. (1996) Simulation Seismic Wave Propagation in 3D Elastic Media Using Staggered-Grid Finite Differences, Bull. Seism. Soc. Am., Vol.86, No.4, 1091-1106, 1996.